Climate Forecast Applications Network (CFAN)

Summer 2019 Temperature Forecast for the U.S.

May16, 2019

Forecast Summary

CFAN's May 2019 summer temperature forecast calls for warm conditions over the western U.S. from May-June-July (MJJ) through July-August-September (JAS), and cool conditions in areas of the eastern and central U.S. during the same period. August-September-October (ASO) forecasts call for warm conditions in the East-Southeast, and suggest cool conditions with lesser confidence in the West.

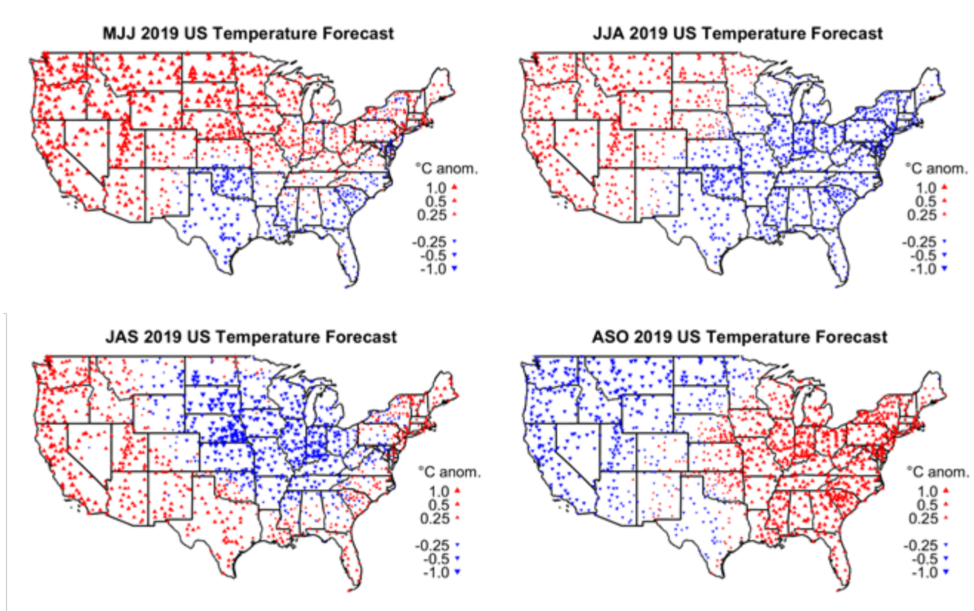

Region	REG	MJJ	JJA	JAS	ASO
Northeast	NE	+0.1	-0.1	+0.1	+0.3
Southeast	SE	0	-0.1	0	+0.4
Midwest	MW	+0.2	-0.1	-0.3	+0.3
South Central	SC	-0.2	-0.2	+0.1	+0.1
Plains/Rockies	PR	+0.5	+0.1	-0.1	-0.1
Northwest	NW	+0.6	+0.2	+0.3	-0.2
Southwest	SW	+0.5	+0.2	+0.4	-0.2

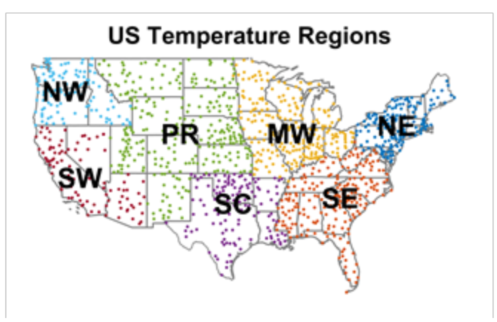

Figure 1. Local and regional temperature forecasts for MJJ, JJA, JAS and ASO 2019 (top panels; C anomalies, 2001-2018 baseline). Local forecasts are shown for 1218 station sites in the U.S. Historical Climatology Network (USHCN) and 7 regions (lower panels).

Background

CFAN's seasonal temperature forecasts project 3-month temperature anomalies over 7 U.S. regions and the 1218 local sites represented in the U.S. Historical Climatology Network (Fig. 1). The current May 2019 forecast predicts seasonal temperature anomalies out to 6 months based on climate observations through April at leads of 3 to 5 months.

Seasonal U.S. temperature 'modes' are defined by the three leading Principal Components (PCs) of monthly USHCN station temperature anomalies. Forecasts are then based on patterns of antecedent circulation anomalies associated with these seasonal temperature modes and their expression in recent observations. Seasonal temperature variability is typically dominated by a single leading mode (PC1, or UST1) that describes coherent variability over the East-Central U.S. and typically >50% of total station temperature variance, while the three leading seasonal modes together capture a large fraction of overall US seasonal temperature variance (typically exceeding 80%).

Climate precursors to these leading temperature PC indices and patterns are identified using a data mining approach based on gridded sea surface temperatures (SSTs) and NCEP-NCAR Reanalysis atmospheric data that are analyzed regionally and globally at 17 vertical levels from the surface to the stratosphere. Correlation maps are first calculated to identify relationships between temperature PC indices and climatic-atmospheric conditions during prior months. Precursor patterns showing strongest correlations, or hindcast relationships with temperature PC indices, are then further screened for forecast skill based on 'leave-one-out' experiments that emulate the actual forecast process.

Recent climate anomalies

Recent global conditions during spring (FMA) 2019 feature persistent El Nino conditions in the tropics, with a Nino 3.4 SST anomaly of +0.7°C, and warm SSTs that extend to most of the northeast Pacific and northwest Atlantic. Tropical sea-level pressure (SLP) anomalies also display a typical El Niño pattern of low pressure in the eastern Pacific and contrasting positive SLP anomalies over the equatorial Atlantic and Indo-Pacific regions (Figure 2). Over the Northern Hemisphere, a deep surface low over the Siberian Arctic, contrasts with high pressure throughout the midlatitudes, an FMA pattern resembling the negative phase of the Arctic Oscillation.

Figure 3 illustrates the recent evolution of global ocean-atmosphere conditions in monthly anomalies of 500 hPa geopotential heights (Z500, left), 1000 hPa near-surface air temperatures (T1000, center) and sea surface temperatures (SSTs, right). Z500 and SST anomalies remained largely unchanged from February through April, with elevated geopotential heights over the tropics reflecting warm tropospheric conditions due largely to El Niño surface warmth. Surface temperature (T1000) anomalies over the Northern Hemisphere show general warmth at high latitudes during April, replacing February and March patterns of sharp temperature contrasts that included unusually cool conditions over much of the continental U.S. as extreme warmth prevailed over Alaska and much of Asia.

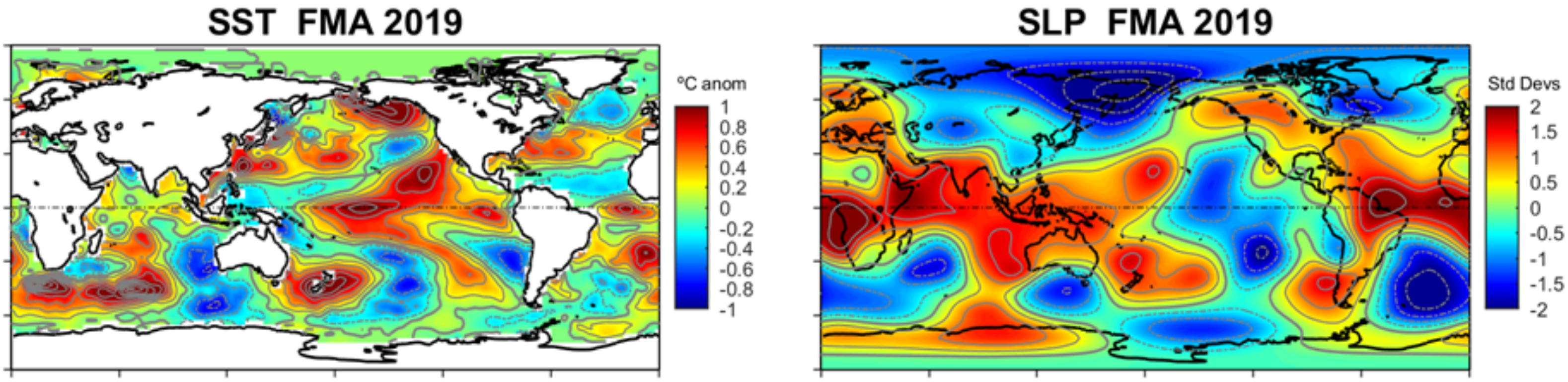

Figure 2. Recent global anomalies of sea surface temperatures (SSTs, left) and atmospheric sea-level pressure (SLP, right) during FMA 2019.

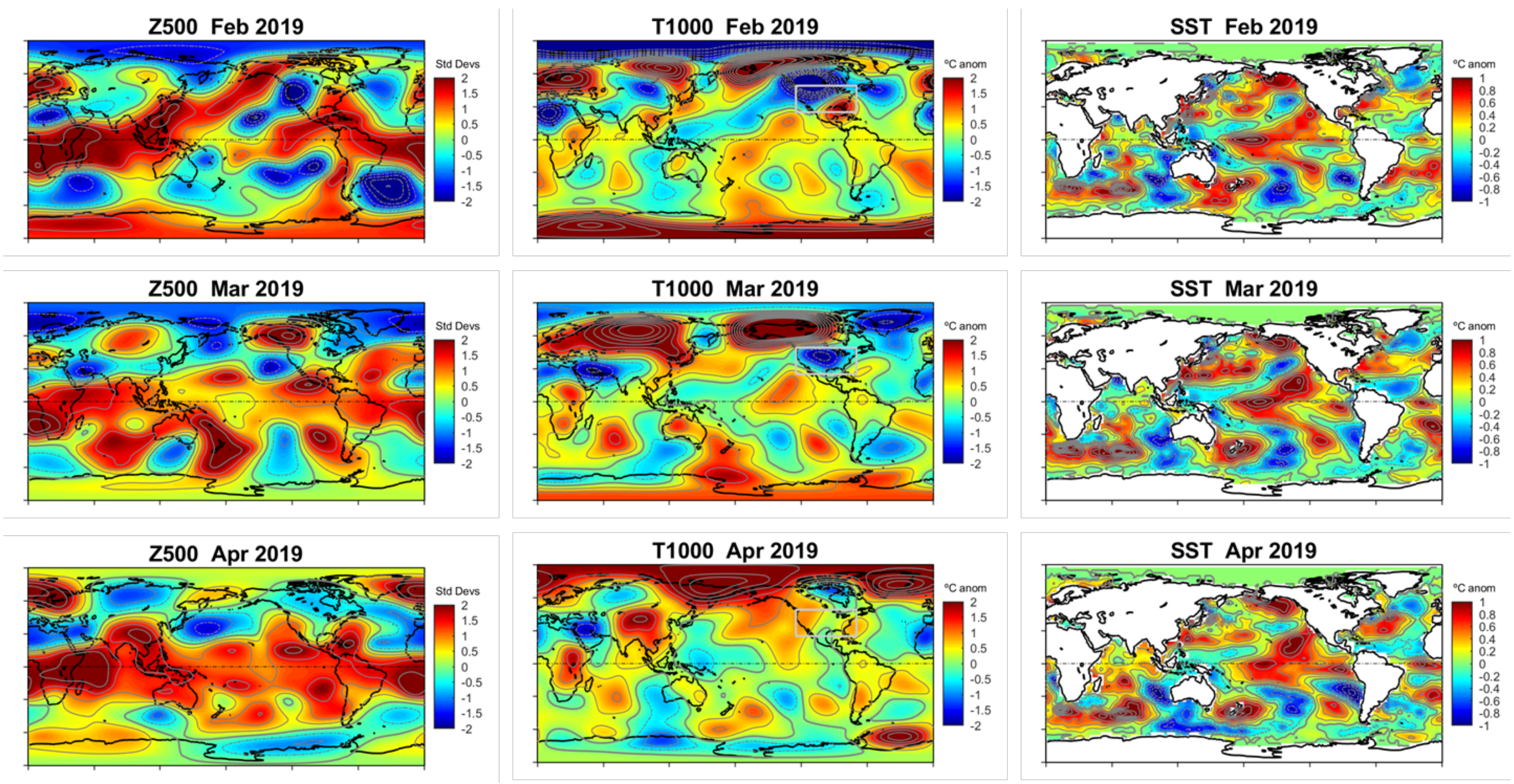

Figure 3. Recent global anomalies of 500 hPa geopotential heights (Z500, left), near-surface air temperatures (T1000, center), and sea surface temperatures (SSTs, right) From February through April 2019.

Warm tropical and northeast Pacific SSTs in spring, as currently observed, are typically followed by warm summer conditions over the northwestern U.S. Throughout most of the U.S., however, a similar temperature response does not typically appear until the early fall window from August to October.

Strong spatial coherence of U.S. summer temperature variability since 2001 can been seen in the similar evolution of JJA and JAS temperature indices for regions of the Northeast, Southeast, Midwest, South-Central and Rockies-Plains (Fig. 4). This common behavior, represented by seasonal temperature PC1 patterns is characterized by a quasi-regular alternation of warm and cool anomalies on a ~4-5 year cycle since 2001. While the 4-5 year time scale is consistent with that of ENSO, mid-summer temperature variations over the East-Central U.S. show generally weak responses to tropical SSTs.

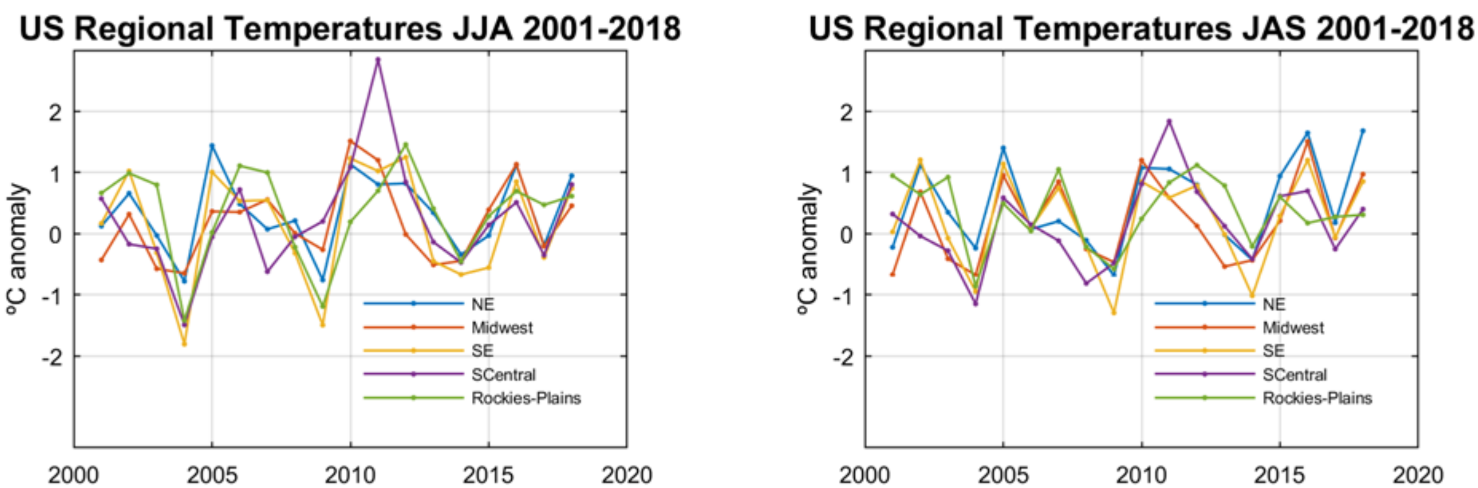

Figure 4. Regional U.S. temperature indices for JJA and JAS, 2001-2018. Coherent variability on a 4-5 year time scale is evident from the Rocky Mountains eastward.

Summer temperature variability over the East-Central U.S. is more heavily influenced by atmospheric circulation anomalies over the extratropical Northern Hemisphere, as seen in correlations of JJA and JAS temperature indices with 500 hPa zonal (U) winds (Figure 5, top panels). Anomalous summer warmth over the East-Central U.S. tends to occur with a northward displacement of westerly winds over the U.S. and the broader NH, reflected by a narrow band of positive U-wind-temperature correlations along 60°N and negative correlations along 30°N. Temperature correlations with U-winds in the lower stratosphere display similar, but more sharply-defined zonal features with similar structures apparent in both the Northern and Southern Hemispheres, suggesting that summer temperature variability over the U.S. is significantly influenced by stratospheric circulation anomalies at hemispheric to global scales with particular impacts over North America.

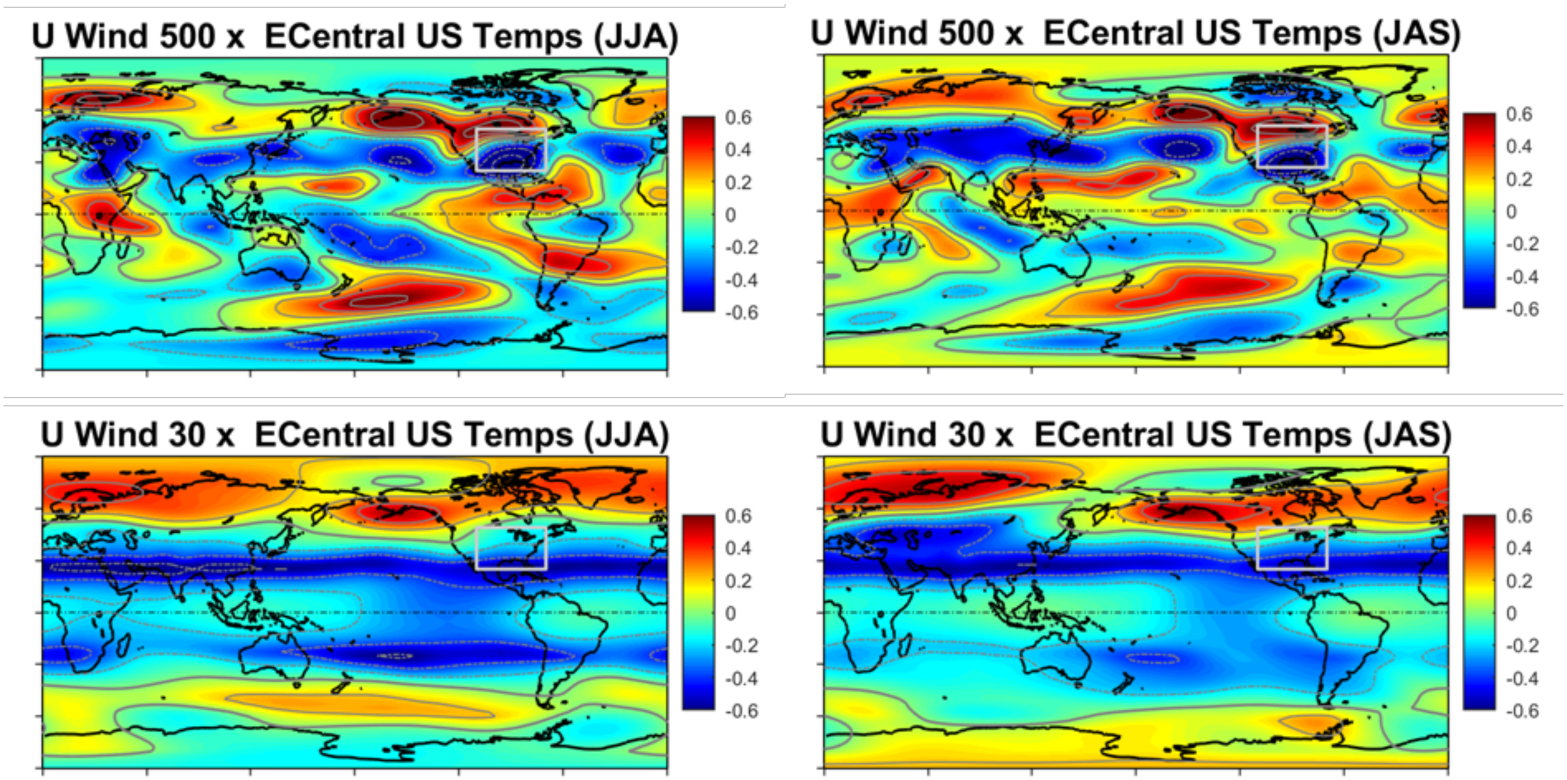

Figure 5. Correlations of East-Central U.S. temperature indices (JJA and JAS) with simultaneous zonal (U) winds in the middle troposphere (500 hPa, upper panels) and the lower stratosphere (30 hPa lower panels). Bands of opposite correlations over the Northern Hemisphere and the U.S. indicate temperature sensitivity to N-S displacements of stratospheric wind anomalies with influence on tropospheric circulation beneath.

Figure 6 illustrates JJA composites of zonal-mean U wind anomalies during warm and cool JJA conditions over the East-Central U.S. Warm and cool summers are distinguished primarily by U wind anomalies from the surface to the lower stratosphere around 30N, consistent with the correlation maps in Figure 5 At lower-stratospheric levels (70 to 50 hPa), anomalous winds at 30N display coupling with tropical zonal winds from 20°N to 20°S, which vary predominantly with the ~28 month Quasi-biennial Oscillation (QBO). While QB variability is not strongly apparent in the JJA and JAS temperature indices, QBO involvement may contribute to the quasi-cyclic appearance of recent temperature variations at twice the QBO period. While additional factors contribute to summer NH circulation anomalies, westerly (positive zonal) QBO wind anomalies at 70 and 50 hPa are poised to intensify during the next several months, suggesting a QBO contribution to anomalous westerly winds over the subtropical NH and cool mid-summer conditions over the East-Central U.S., based on patterns observed over the past two decades.

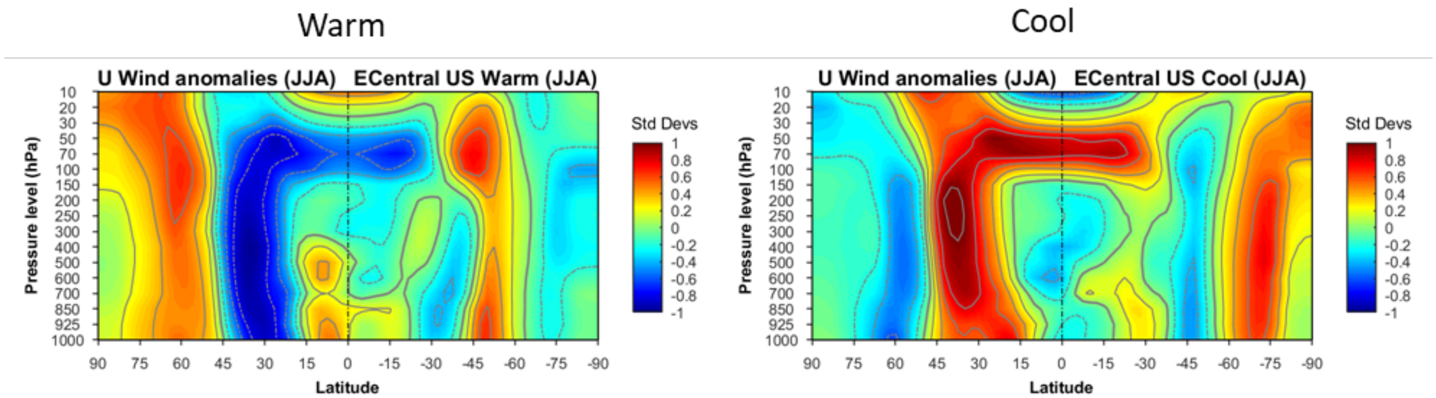

Figure 6. Zonal wind anomaly composites by latitude (x-axis) and height (y-axis) for warm and cool JJA seasons over the East-Central U.S. Deep zonal wind anomalies display coupling with equatorial stratospheric winds of the equatorial 28-month Quasi-biennial Oscillation (QBO).

Temperature predictors

Our forecast approach is based on objective detection of atmospheric and SST precursor patterns that skillfully predict large-scale U.S. temperature PC patterns in historical forecast experiments. Forecasts are designed to anticipate future anomalies of the leading three U.S. temperature PC indices and associated patterns of temperature anomalies based on recent atmosphere-ocean conditions and tendencies.

A variety of atmospheric indicators suggest modestly cool conditions over the East-Central U.S. from MJJ to JAS, consistent with QBO indications discussed above. During the same seasonal windows, PC3 temperature indices show evidence of a 10-20 year trend toward cooler conditions in the Midwest and warming elsewhere, behavior that is suggested to continue in 2019 by most forecast models, with strongest indications for cool Midwest conditions in JAS.

In early fall (ASO), U.S. temperatures show stronger connections to tropical ocean-atmosphere anomalies from the previous spring. Warm conditions over the East-Central U.S. are suggested by current El Nino SST anomalies and broader warmth throughout the tropical troposphere. Figure 7 illustrates an ASO PC1 forecast pattern (top right) that matches current observations of elevated 200 hPa geopotential heights in the tropics (bottom left), which contribute to a forecast of warm ASO conditions over the eastern two-thirds of the U.S. (right panel). Greatest ASO warmth is projected for the Southeast, where SST responses are particularly strong. Some uncertainty stems from currently neutral SST anomalies in the tropical North Atlantic, which are typically warm in the aftermath of a winter El Nino. A small number of models suggest cool conditions in the west during ASO; however, this forecast is inconsistent with warm NE Pacific SSTs that are currently in place and likely to persist with an expectation of ongoing El Nino conditions. While most models point to modestly cool conditions in the eastern half of the country from MJJ to JAS, models show differences in the seasonal timing and regional position of expected modest cool anomalies. Forecast details for all seasonal temperature PCs are shown in the Appendix.

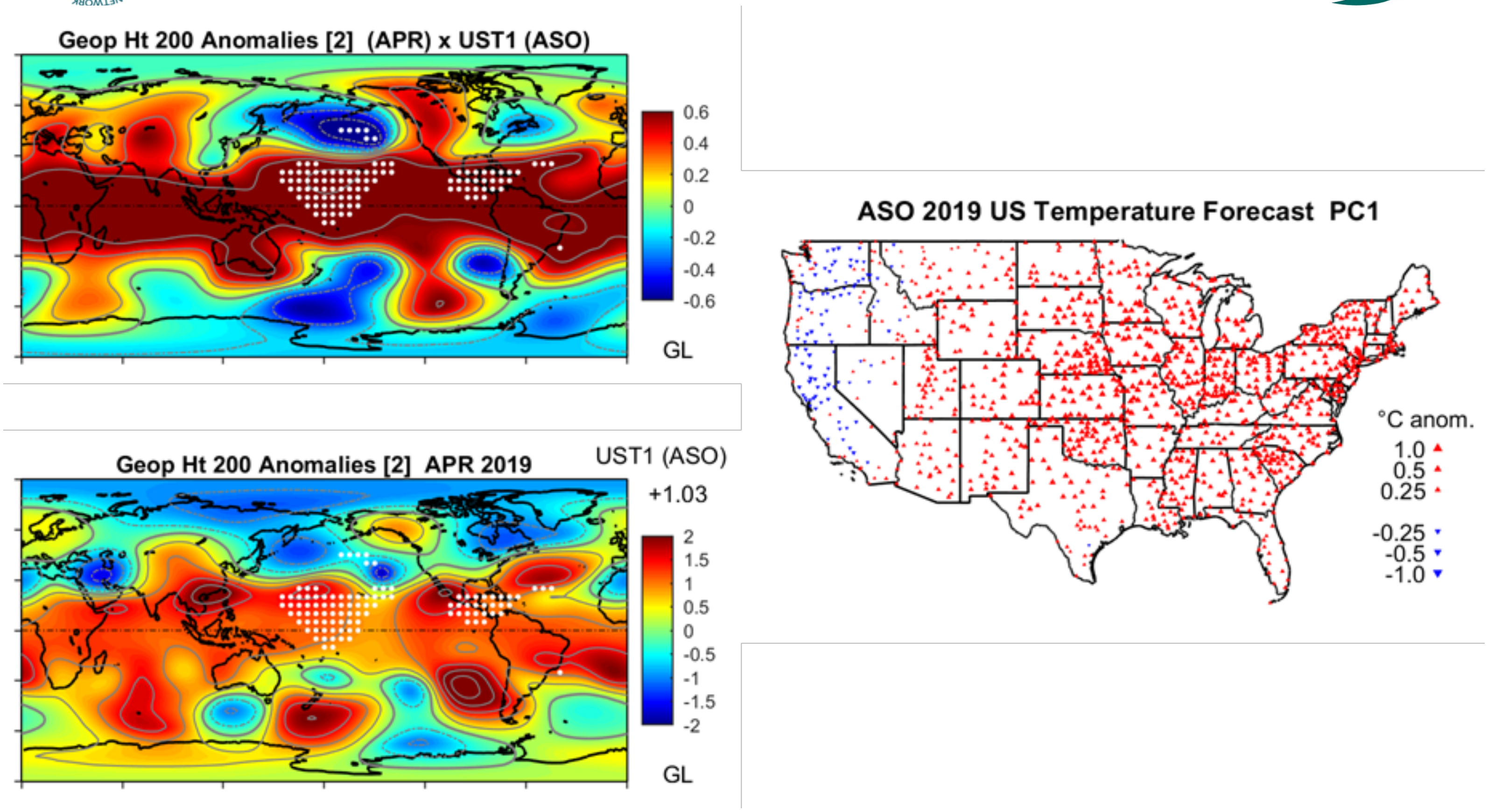

Figure 7. Forecast patterns for US temperature PC1 (ASO). Top left panel shows correlations of March-April 200 hPa geopotential heights (Z200) with the ASO PC1 temperature index (see appendix). Hatched areas mark local Z200 anomalies with strongest forecast skill. Lower left panel illustrates recent March-April Z200 anomalies (in standard deviations) with the same hatching, which contribute to a forecast of warm ASO conditions in the structure of the PC1 pattern (right panel).

Appendix: Forecast details

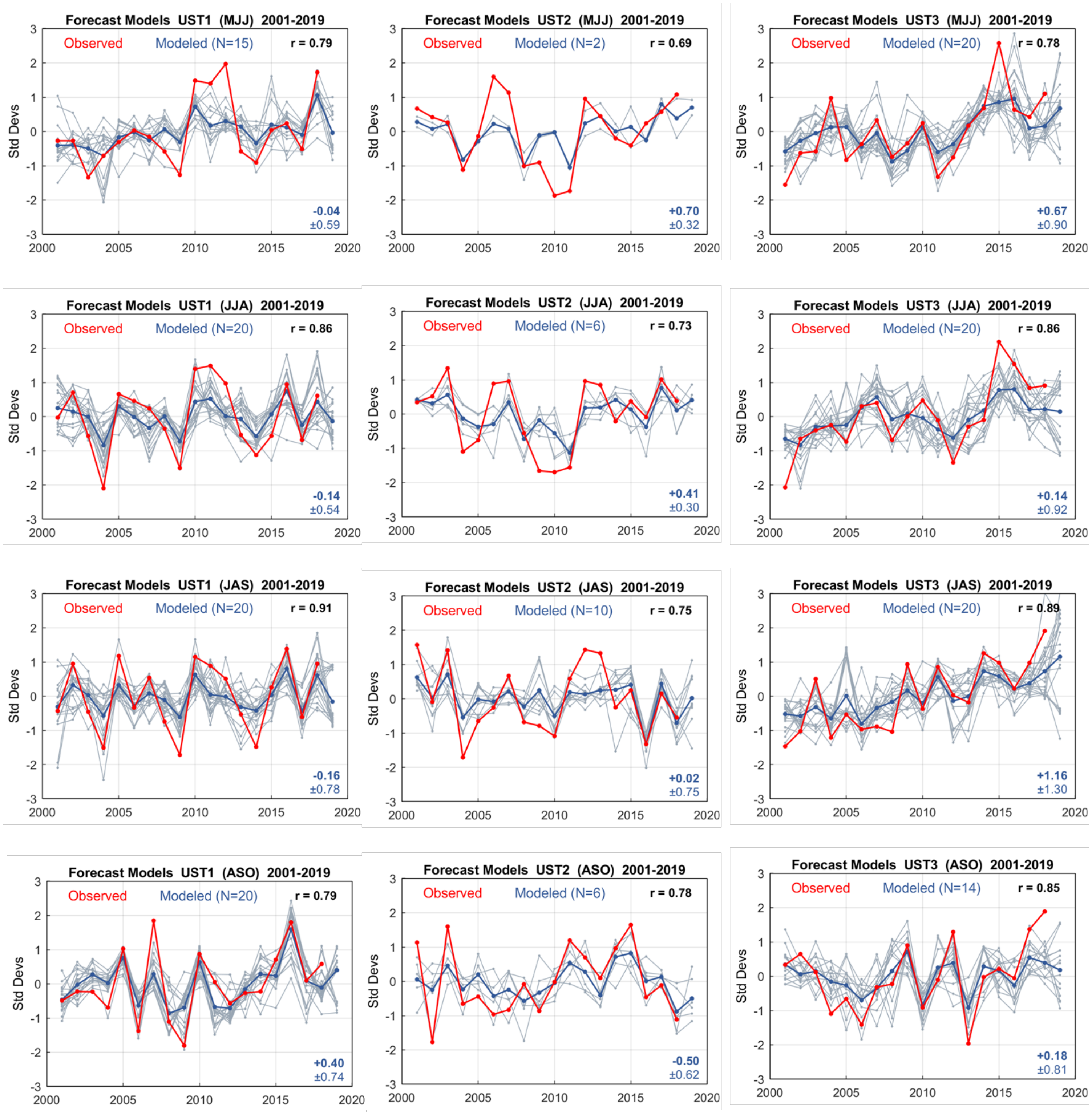

Figure A1. Forecasts of the leading 3 U.S. temperature PC indices (blue) and observed PC anomalies (red) for MJJ, JJA, JAS and ASO (top to bottom).

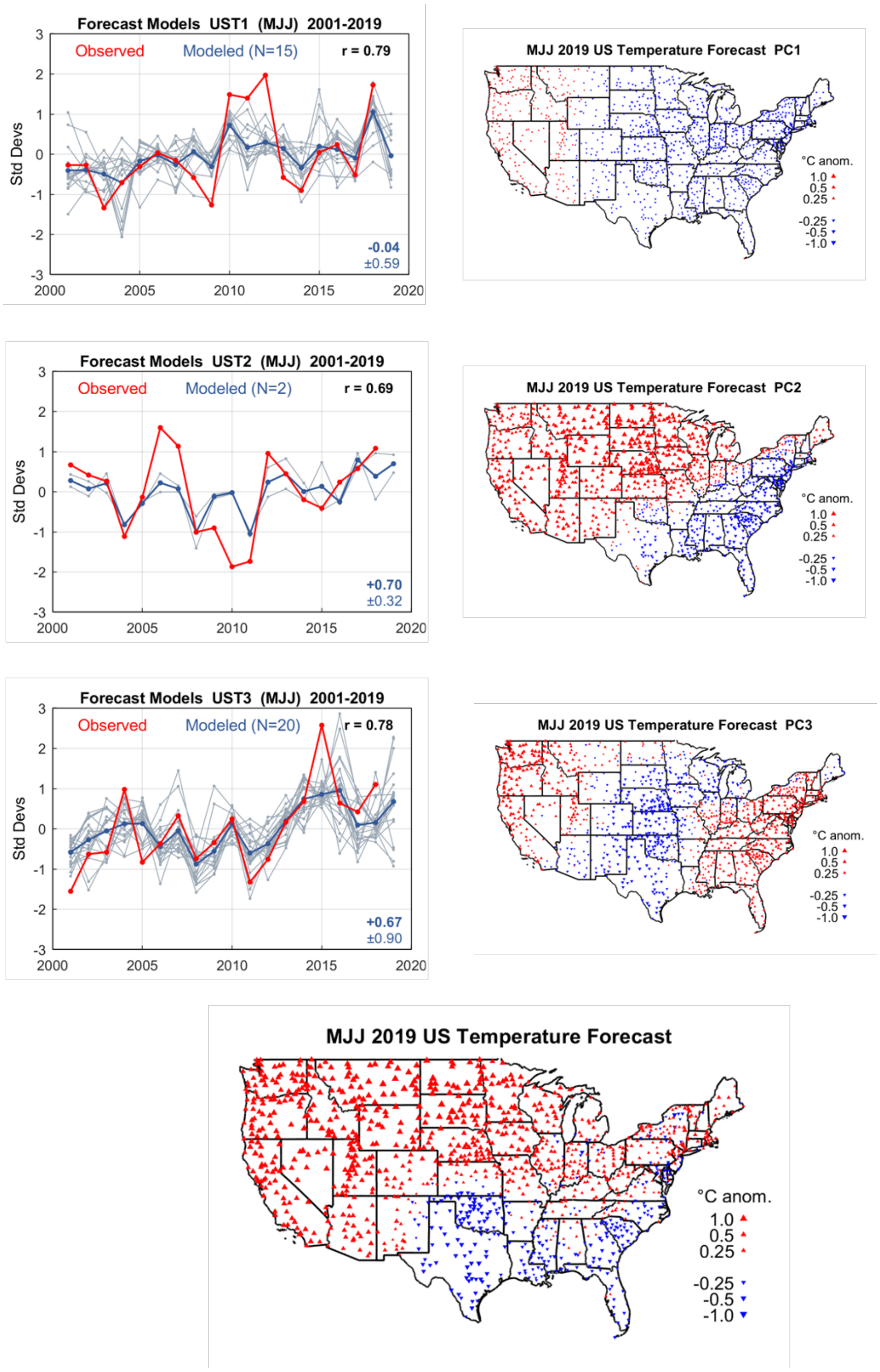

Figure A2. Overall MJJ 2019 temperature forecast (bottom) and historical and current forecasts of the three leading U.S. temperature PC indices (left). Observed US temperature PC index anomalies (red) are compared to historical model forecasts (means shown in blue). Final forecast values (blue) represent PC index forecasts for MJJ 2019, noted in bottom right with ±1 standard deviation uncertainty. Individual model forecasts are shown by fine gray lines. Forecasts are presented as °C anomalies relative to 2001-2018.

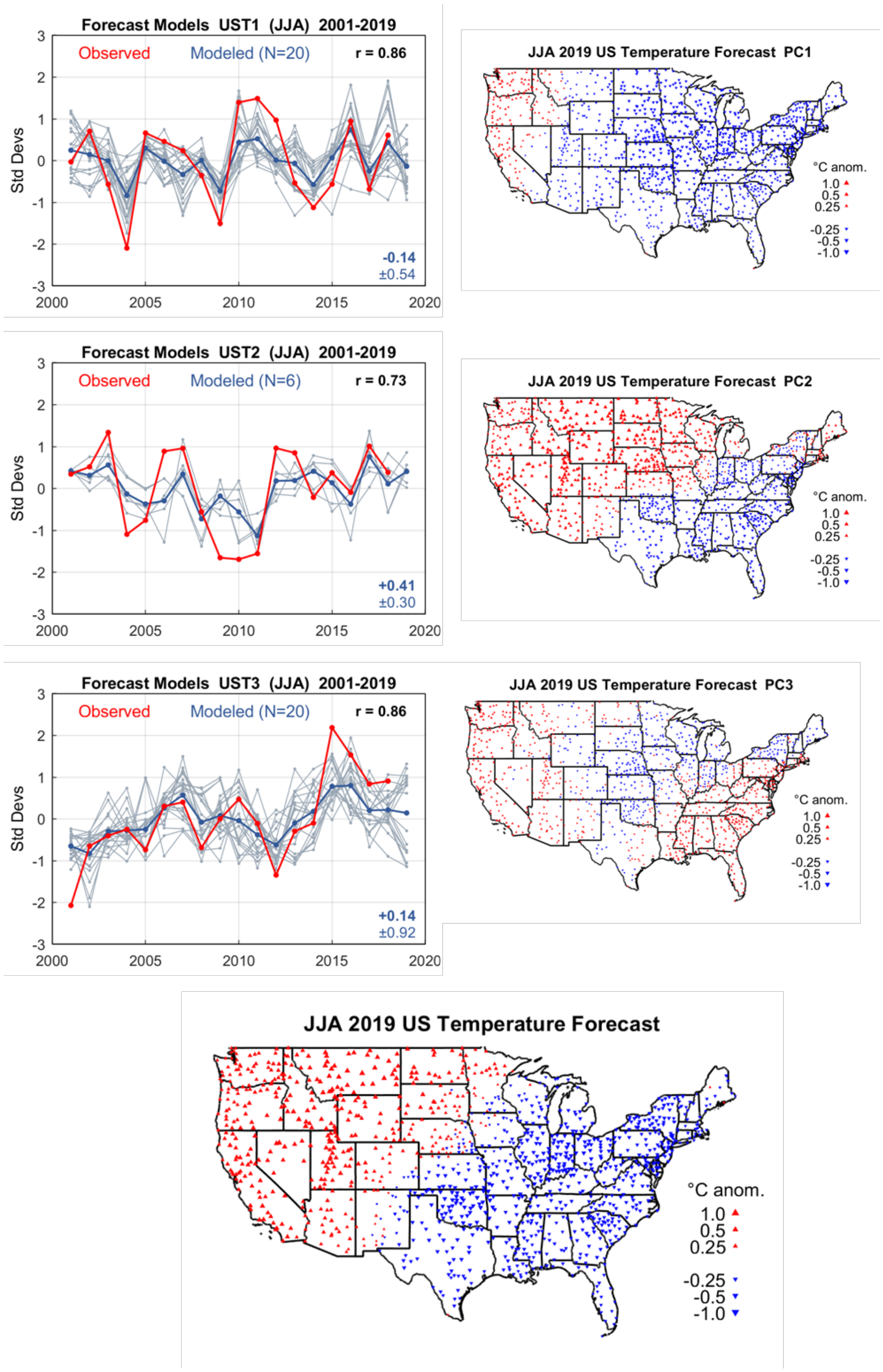

Figure A3. JJA 2019 U.S. temperature forecast (bottom) and PC-based forecast models (same as Fig. A2).

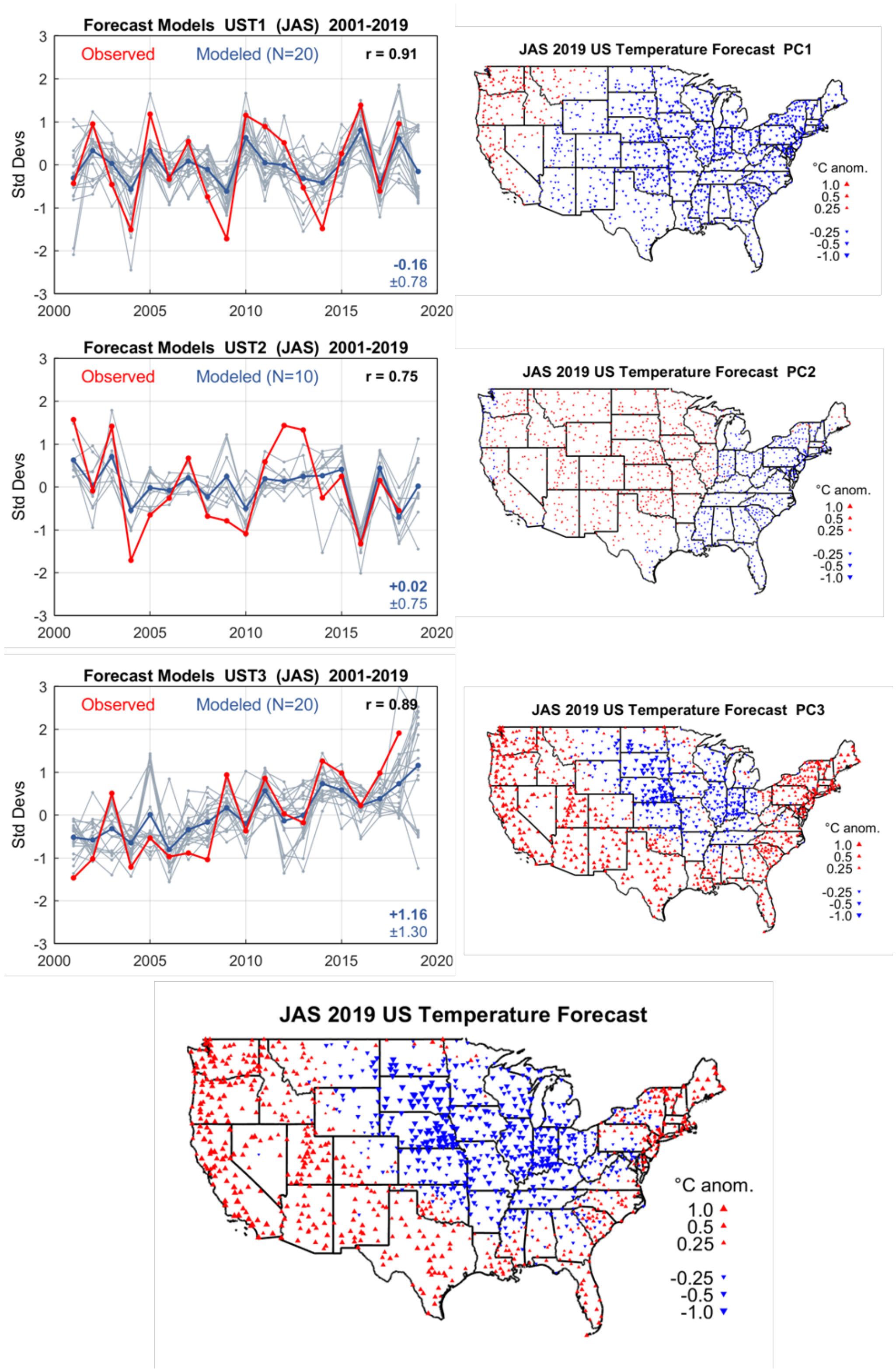

Figure A4. JAS 2019 U.S. temperature forecast (bottom) and PC-based forecast models (same as Fig. A2).

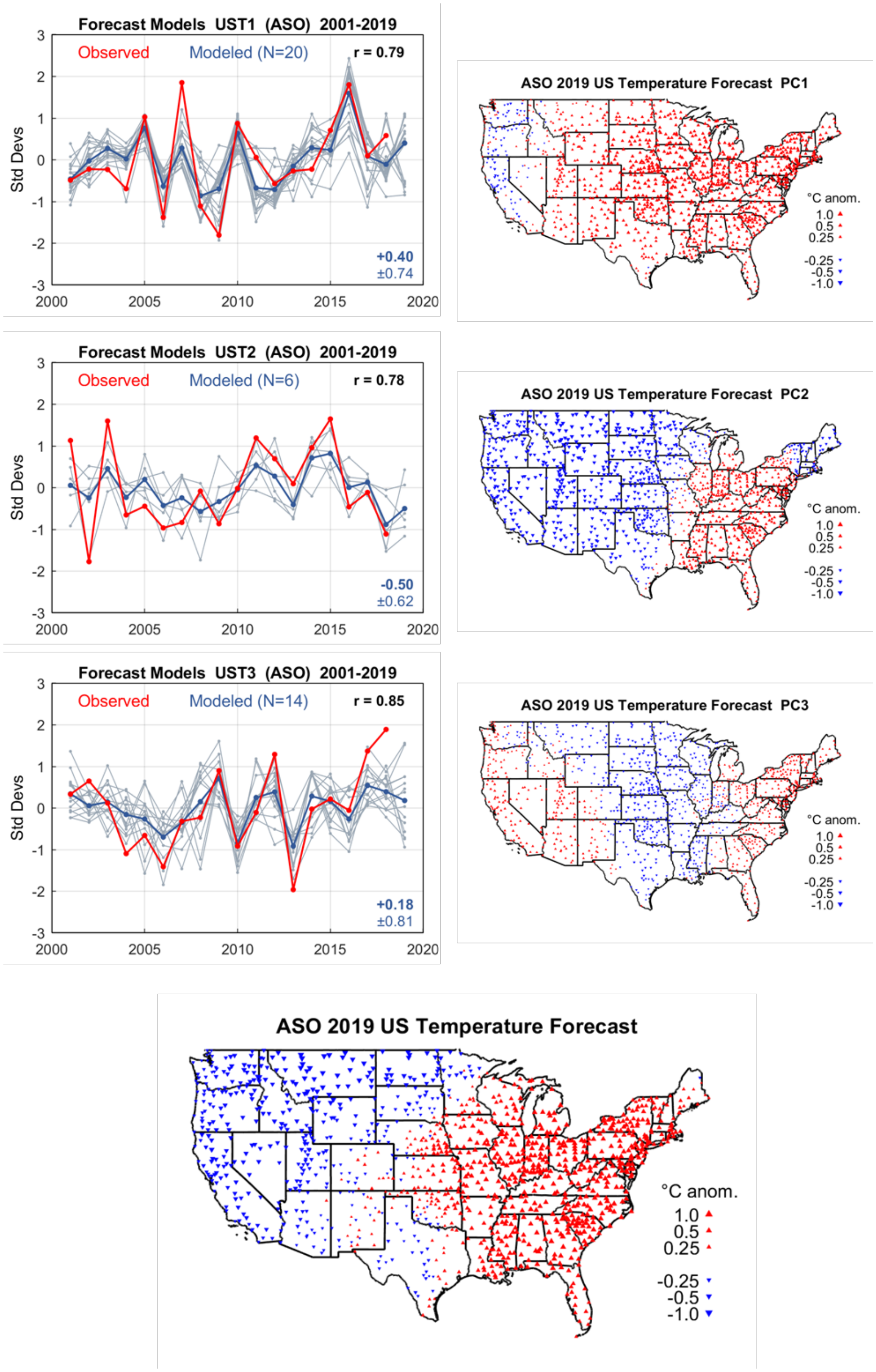

Figure A5. ASO 2019 U.S. temperature forecast (bottom) and PC-based forecast models (same as Fig. A2).